

Effects of Cholesterol on Surface Activity and Surface Topography of Spread Surfactant Films[†]

Robert V. Diemel,^{‡,§} Margot M. E. Snel,^{||} Lambert M. G. van Golde,[‡] Günther Putz,[§] Henk P. Haagsman,^{‡,⊥} and Joseph J. Batenburg^{*,‡}

Departments of Biochemistry and Cell Biology and of Science of Food of Animal Origin, Graduate School of Animal Health, Faculty of Veterinary Medicine, Utrecht University, P.O. Box 80176, 3508 TD Utrecht, The Netherlands, Department of Anesthesiology and Critical Care Medicine, The Leopold-Franzens-University of Innsbruck, Anichstrasse 35, A-6020 Innsbruck, Austria, and Department of Interfaces, Faculty of Chemistry, Utrecht University, Padualaan 8, 3584 CH Utrecht, The Netherlands

Received February 7, 2002; Revised Manuscript Received August 6, 2002

ABSTRACT: Pulmonary surfactant forms a monolayer of lipids and proteins at the alveolar air/liquid interface. Although cholesterol is a natural component of surfactant, its function in surface dynamics is unclear. To further elucidate the role of cholesterol in surfactant, we used a captive bubble surfactometer (CBS) to measure surface activity of spread films containing dipalmitoylphosphatidylcholine/1-palmitoyl-2-oleoylphosphatidylcholine/1-palmitoyl-2-oleoylphosphatidylglycerol (DPPC/POPC/POPG, 50/30/20 molar percentages), surfactant protein B (SP-B, 0.75 mol %), and/or surfactant protein C (SP-C, 3 mol %) with up to 20 mol % cholesterol. A cholesterol concentration of 10 mol % was optimal for reaching and maintaining low surface tensions in SP-B-containing films but led to an increase in maximum surface tension in films containing SP-C. No effect of cholesterol on surface activity was found in films containing both SP-B and SP-C. Atomic force microscopy (AFM) was used, for the first time, to visualize the effect of cholesterol on topography of SP-B- and/or SP-C-containing films compressed to a surface tension of 22 mN/m. The protrusions found in the presence of cholesterol were homogeneously dispersed over the film, whereas in the absence of cholesterol the protrusions tended to be more clustered into network structures. A more homogeneous dispersion of surfactant lipid components may facilitate lipid insertion into the surfactant monolayer. Our data provide additional evidence that natural surfactant, containing SP-B and SP-C, is superior to surfactants lacking one of the components, and furthermore, this raises the possibility that the cholesterol found in surfactant of warm-blooded mammals does not have a function in surface activity.

Pulmonary surfactant is a mixture of lipids and proteins, synthesized and secreted by the alveolar type II epithelial cells. Its main function is to reduce the surface tension at the alveolar air/liquid interface. This is achieved by formation of a surface-active film that consists of a lipid monolayer highly enriched in dipalmitoylphosphatidylcholine (DPPC)¹ and a bilayer or multilayer structures (surface-associated reservoir) closely attached to the monolayer. The presence

of a surfactant film prevents the alveoli from collapsing at end-expiration and makes breathing with minimal effort possible. The existence of such a film has been visualized in vitro by atomic force microscopy (AFM) and fluorescence light microscopy (1) and in vivo by electron microscopy (2). Film compression during expiration might lead to a squeeze-out of non-DPPC (3, 4), film expansion during inspiration to selective adsorption of DPPC (2), or just to an alteration of structure rather than a change in composition (1, 5, 6).

Important components for surfactant film formation and homeostasis are the small hydrophobic surfactant-specific proteins B and C (SP-B and SP-C). SP-B is a 79 amino acid amphipathic protein that is active as an 18 kDa dimer (7). SP-B has a net positive charge that is thought to be essential for its interaction with negatively charged phospholipids (8–10). The many different activities ascribed to SP-B include the ability to induce the formation of a monolayer film from vesicles (11), to facilitate respreading of films from the collapsed phase (12), to support membrane fusion and lysis (13), to aid in the formation of tubular myelin (14), and to increase surfactant reuptake by type II cells (15). In addition, recent studies carried out with a captive bubble surfactometer (CBS) suggested that SP-B induces film refinement by

[†] The authors received financial support from the Fonds zur Förderung der Wissenschaftlichen Forschung FWF (R.V.D. and G.P.) and the European Commission (J.J.B. and H.P.H.).

* Corresponding author: Fax +31-30-2535492; e-mail J.J.Batenburg@vet.uu.nl.

[‡] Department of Biochemistry and Cell Biology, Utrecht University.

[§] The Leopold-Franzens-University of Innsbruck

^{||} Department of Interfaces, Utrecht University.

[⊥] Department of the Science of Food of Animal Origin, Utrecht University.

¹ Abbreviations: AFM, atomic force microscopy; CBS, captive bubble surfactometer; DPPC, 1,2-dipalmitoyl-*sn*-glycero-3-phosphocholine; EDTA, ethylenediaminetetraacetic acid; HEPES, *N*-(2-hydroxyethyl)-1-piperazine-*N'*-2-ethanesulfonic acid; PBS, pulsating bubble surfactometer; POPC, 1-palmitoyl-2-oleoyl-*sn*-glycero-3-phosphocholine; POPG, 1-palmitoyl-2-oleoyl-*sn*-glycero-3-phospho-*rac*-(1-glycerol); SP-B, surfactant protein B; SP-C, surfactant protein C; SUV, small unilamellar vesicles.

selective removal of non-DPPC lipid upon cycling (16). The importance of SP-B is further documented by the observation that homozygous SP-B knockout mice died of respiratory failure immediately after birth (17). Moreover, blocking of SP-B with monoclonal antibodies in rabbits led to respiratory failure and the loss of surfactant activity (18).

SP-C is a 35 amino acid protein that is extremely hydrophobic. It is further characterized by one or two palmitoylated cysteines in its N-terminal part. The C-terminal amino acids form an α -helix rich in valines (19). In a lipid environment the α -helical content increases and might even extend to the two palmitoylated cysteines. The activities of SP-C largely overlap those of SP-B, including promotion of lipid adsorption into the air/liquid interface (20), stabilization of the monolayer film (21), respreading of films from the collapsed phase (12), and surfactant reuptake by type II cells (15). Upon compression of a lipid monolayer to a surface tension of 22 mN/m, SP-C has been shown to induce formation of protrusions with heights that are multiples of lipid bilayers (1). Surplus surfactant might be kept in close proximity to the monolayer in these protrusions, from which it might be inserted quickly back into the monolayer upon inspiration. In contrast to SP-B knockout mice, SP-C knockout mice survive, although their surfactant shows altered stability when measured in small captive bubbles (22).

Lipids are the main components of surfactant (see ref 23 for review). Most abundant and best characterized are the phospholipids DPPC and phosphatidylglycerol (PG). DPPC (40–50 wt % of the lipid pool) is responsible for keeping the surface tension near zero during compression. Negatively charged PG (5–10 wt %) is likely to interact with positive charges of SP-B and SP-C. The most important nonphospholipid in surfactant is cholesterol, present in amounts of 10–20 mol % (approximately 5–10 wt %) (24). Even though the presence of cholesterol in surfactant has long been recognized, little is known about its function. Although it is presumed that, in the presence of the hydrophobic surfactant proteins, cholesterol is important for enhancing lipid adsorption into the monolayer, studies with a Langmuir–Wilhelmy surface balance (25, 26) or pulsating bubble surfactometer (PBS) (27) showed that cholesterol also had deleterious effects, like increasing the minimum surface tension during compression or diminishing postcollapse respreading. In pure lipid mixtures, cholesterol has been shown to be beneficial by enhancing surface reentry and respreading of the monolayer upon dynamic compression beyond collapse, as measured by Wilhelmy balance (28).

To further elucidate the role of cholesterol in surfactant films, we studied the effect of cholesterol on (i) the minimum and maximum surface tensions under dynamic conditions in a CBS and (ii) the topography of the surface-associated reservoir by AFM. For this purpose, we compared mixtures of lipids (DPPC, POPG, POPC) and proteins (SP-B and/or SP-C) with and without cholesterol.

EXPERIMENTAL PROCEDURES

Materials. 1,2-Dipalmitoyl-*sn*-glycero-3-phosphocholine (DPPC), 1-palmitoyl-2-oleoyl-*sn*-glycero-3-phosphocholine (POPC), 1-palmitoyl-2-oleoyl-*sn*-glycero-3-phospho-*rac*-(1-glycerol) (POPG), and cholesterol were obtained from Avanti Polar Lipids (Alabaster, AL); HEPES was purchased from

Life Technologies (Paisley, Scotland); EDTA and CaCl₂ were obtained from Baker Chemicals (Deventer, The Netherlands); chloroform (CHCl₃) and methanol (MeOH) from Labscan (Dublin, Ireland) were HPLC-grade.

Biochemical Assays. Bovine SP-B and porcine SP-C obtained from lung lavage were isolated and characterized according to standard procedures (29). The protein concentration was determined by fluorescamine assay (30). Concentrations of phospholipids (31) and cholesterol (32) were determined as described.

Vesicle Preparation. Small unilamellar vesicles (SUV) were prepared as follows. Aliquots of lipids from stock solutions in CHCl₃/MeOH were dried under a continuous stream of nitrogen at room temperature. The resulting dry lipid film was rehydrated by addition of subphase buffer (140 mM NaCl, 10 mM HEPES, 0.5 mM EDTA, and 2.5 mM CaCl₂, pH 6.9), vortexing, and incubation at 55 °C for 15 min. The multilamellar vesicles thus formed were sonicated five times for 20 s at 2 μ m amplitude at 55 °C with 20 s intervals to obtain SUV. The SUV were cooled to 37 °C and used immediately.

Captive Bubble Surfactometry. The capability of the hydrophobic surfactant proteins to insert lipids into the air/liquid interface and to alter the lipid composition of this layer was determined by use of a pressure-driven CBS (33, 34). We used a CBS since it has several advantages over PBS or Wilhelmy balance (33, 35), especially when making dynamic compressions with spread film in which the composition is known (34). In short, a bubble (0.50 cm²) was formed in subphase buffer by injecting air (28.5 μ L) into the sample chamber at 1.0 bar and 37 °C. After that, a surfactant film containing 0.25 nmol of lipids with or without hydrophobic surfactant proteins was spread at the air/liquid interface by use of a glass syringe (volume of 0.05 μ L). Subsequently, the subphase was stirred for 30 min to enhance desorption of solvent. Next, the sample chamber was perfused for 20 min with 10 times the subphase volume. Thereafter, 100 μ L portions of SUV of various lipid compositions (see below) were injected into the subphase (final concentration of 1 μ mol of lipid/mL), and stirring was continued for another 15 min. To study adsorption, the bubble area was increased by sudden lowering of the pressure to 0.5 bar, where it was kept for 10 s. Subsequently, the pressure in the sample chamber was cycled five times within 1 min between two preset pressures of 0.5 and 2.8 bar to measure surface activity during dynamic cyclic compression and expansion of the bubble. The system pressure was kept constant (2.8 bar) at the end of the fifth compression over a period of 5 min to determine film stability. Finally, the pressure was cycled another five times and film stability was measured again. A video camera continuously monitored the shape and size of the bubble from which the surface tension values were calculated. During each second 25 video frames were generated. Maximum surface tension was defined as the surface tension measured at the end of bubble expansion (just before onset of compression). Minimum surface tension was measured at the end of compression (just before onset of expansion). All measurements were carried out at least in 4-fold.

CBS Film and SUV Composition. When spread films contained protein, concentrations of 0.75 mol % for SP-B and 3 mol % for SP-C were used. These concentrations were shown to have maximal activity in this experimental setup

(34, 36, 37). Films and vesicles were made from a standard phospholipid mixture consisting of DPPC/POPC/POPG (50/30/20 mol %), which was mixed in various ratios with cholesterol (100 mol %). Therefore, a mixture containing for instance 10 mol % cholesterol consisted of DPPC/POPC/POPG/cholesterol (45/27/18/10 mol %). In this way the total amount of lipids was always kept constant.

Atomic Force Microscopy. For Langmuir–Blodgett transfer, films were prepared on a home-built Teflon trough with an operational area of 66.5 cm². The surface tension of the spread monolayer was measured with a platinum Wilhelmy plate connected to a microbalance (Cahn2000, Ankersmit, Oosterhout, The Netherlands). Before film spreading, a freshly cleaved mica sheet was dipped vertically into a subphase of demineralized water at room temperature (20 ± 3 °C). Films, composed of DPPC/POPC/POPG (50/30/20) plus 0.75 mol % SP-B and/or 3 mol % SP-C with or without cholesterol (10 mol %) in CHCl₃/MeOH, were formed by spreading aliquots onto the subphase. After the solvent had been allowed to evaporate for 5 min, the film was compressed at a rate of 8.6% of the operational area per minute, until a surface tension of 22 mN/m was reached. Subsequently, films were transferred onto a disk of mica (14 mm in diameter) at a rate of 2.0 mm/min at constant surface tension.

For AFM measurements, transferred films were mounted on the J-type scanner (150 μm × 150 μm scan range) of a Nanoscope III Multimode microscope (Digital Instruments, Santa Barbara, CA) operating in contact mode in air. Scanning was performed with oxide-sharpened Si₃N₄ tips with a spring constant of 0.12 N/m. Scans were recorded at minimal force and the interaction force was dominated by strong adhesion of usually 15 nN. No indications for tip-induced film damage were found, as checked by zooming out after an area had been scanned.

Statistics. Data are presented as average ± SEM, unless stated otherwise. For statistical analysis, the computer program SPSS version 9.0 was used (SPSS Inc., Chicago, IL). The values of the heights of the protrusions observed with AFM were analyzed by Student's *t*-test. To compare the relative positions of the lines in graphs of minimum and maximum surface tension of CBS films, data were analyzed by repeated measures analysis. In this procedure the data of the lines as a whole (all data points of each line) were compared with each other. Differences were considered significant at *P* < 0.05.

RESULTS

Effect of Cholesterol on Surface Tension: Captive Bubble Surface Tension

CBS experiments were performed on spread films to study the effect of cholesterol on film dynamics. In previous studies we used films and vesicles that had a DPPC content of 80% (36–38), but since hardly any effect of cholesterol on surface tension was noted in preliminary tests on surfactant samples containing such a high DPPC content (results not shown), films and vesicles with a more physiologically relevant DPPC content were used throughout this study: a standard phospholipid mixture of DPPC, POPC, and POPG at a fixed molar percentage of 50/30/20, which was mixed with various amounts of cholesterol.

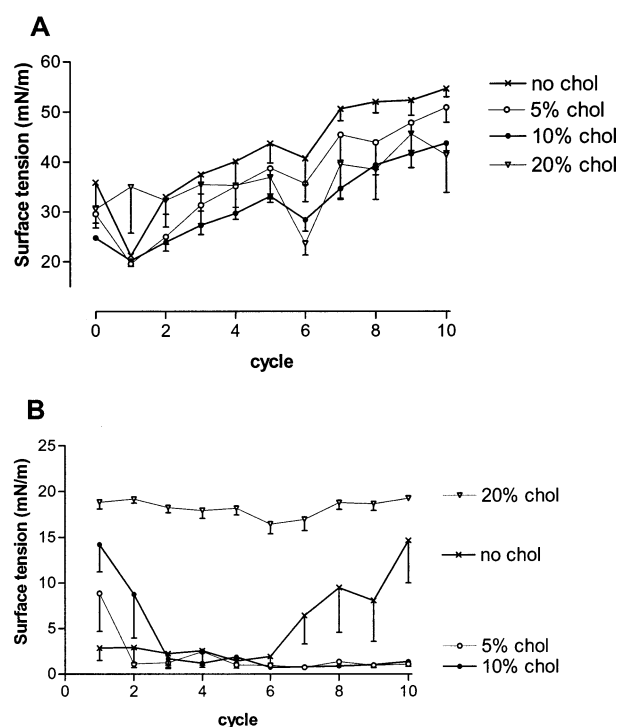


FIGURE 1: Maximum (A) and minimum (B) surface tensions during cycling of spread SP-B-containing films consisting of DPPC/POPC/POPG (50/30/20) mixed in different ratios with 100 mol % cholesterol (chol). The SP-B content of the mixture was 0.75 mol %. The final molar concentrations of cholesterol in the various lipid mixtures is indicated. Protein/lipid mixtures (0.25 nmol), dissolved in CHCl₃/MeOH (1/1 v/v), were spread at the bubble interface in a CBS. After the subphase was washed, SUV were injected; SUV had the same lipid composition as the film but contained no protein. Subsequently, cycling was performed by varying the pressure between 0.5 and 2.8 bar. Values shown are the average of at least four separate experiments ± SEM. Statistical analysis of the data for the maximum surface tension showed that the line for 10 mol % cholesterol differed significantly from that for 0 mol % cholesterol (*P* = 0.013). Other differences between the lines in panel A were not statistically significant.

Effect of Cholesterol in the Presence of SP-B. A concentration curve of cholesterol in films of standard mixture plus SP-B (0.75 mol %) showed that the maximum surface tension (Figure 1A) decreased with increasing cholesterol concentrations, reaching the lowest values at 10 mol % cholesterol (*P* = 0.013). In most experiments, maximum surface tension temporarily decreased during the stability test period at high pressure following the fifth compression. For cholesterol concentrations up to 10 mol %, the minimum surface tension (Figure 1B) reached on the second or third compression was always <5 mN/m, whereas minimum surface tension of films containing 20 mol % cholesterol was always >15 mN/m. Although no statistically significant difference in minimum surface tensions was observed for 0%, 5%, and 10% cholesterol for the first five cycles, initially stable films rapidly destabilized after the fifth compression when no cholesterol was present. The observed increase in minimum surface tension in the absence of cholesterol could indicate an irreversible loss of DPPC from the film.

A film can be enriched in a specific component by bubble cycling when experiments are started with differences in concentration of that particular component between film and subphase. At an initial film concentration of 0 mol %

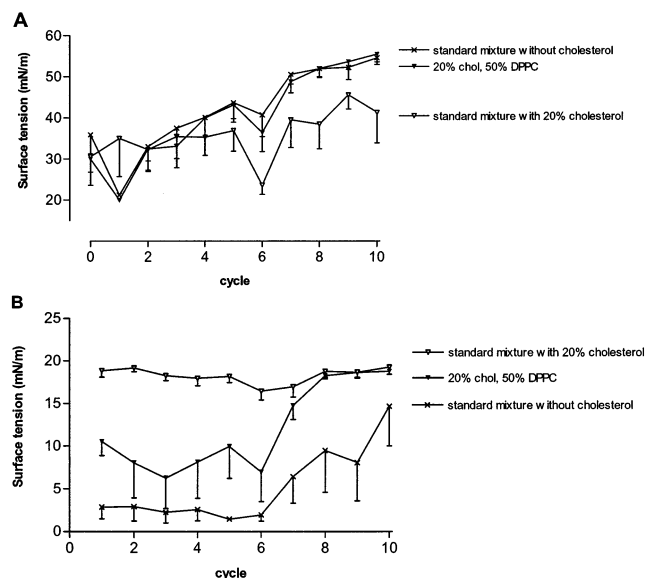


FIGURE 2: Influence of an increased amount of DPPC on maximum (A) and minimum (B) surface tensions during cycling of spread SP-B-containing lipid films. The SP-B content of the mixture was 0.75 mol %. The lipid mixture consisted of the standard phospholipid mixture DPPC/POPC/POPG (50/30/20), which was used either without cholesterol (indicated as standard mixture without cholesterol) or mixed in the ratio 80:20 with 100% cholesterol (indicated as standard mixture with 20% cholesterol), or consisted of DPPC/POPC/POPG/cholesterol (50/10/20/20) (indicated as 20% cholesterol, 50% DPPC). SUV and film had the same lipid composition. Values shown are the average of at least four separate experiments \pm SEM.

cholesterol, the film can be enriched in cholesterol when SUV containing 10 mol % cholesterol are injected into the subphase. Similarly, a dilution of cholesterol in the film can be created by starting the experiments with 10 mol % cholesterol in the film and 0 mol % in the SUV. No significant difference in minimum or maximum surface tension was found between experiments starting with 10 mol % cholesterol in the film only, in the subphase only, or in both the film and the subphase (not shown). From this we conclude that cholesterol is able to adsorb from the subphase into the bubble surface and vice versa.

Although it has been proposed for calf lung surfactant extract measured by CBS (5) and PBS (39) that films are stable even at less than 40% DPPC, we considered the possibility that the effect of 20% cholesterol addition on minimum surface tension (Figure 1B) might actually have been caused by a decrease in the amount of DPPC rather than by the cholesterol addition per se. To investigate the effect of the amount of spread DPPC on surface tension, experiments were performed with a mixture of DPPC/POPC/POPG/cholesterol (50/10/20/20) (Figure 2). In this lipid mixture the concentration of DPPC was truly 50%, instead of 40% as was the case when the standard phospholipid mixture DPPC/POPC/POPG (50/30/20) was mixed with 100% cholesterol in the ratio 80:20. The cholesterol was accommodated by decreasing the amount of POPC to 10%. When 20% cholesterol was present, minimum surface tension reached with the 50/10/20/20 mixture was lower than with the standard phospholipid mixture mixed with 100% cholesterol in the ratio 80:20 ($P = 0.022$) (Figure 2B). However, the 50/10/20/20 mixture never reached the low minimum

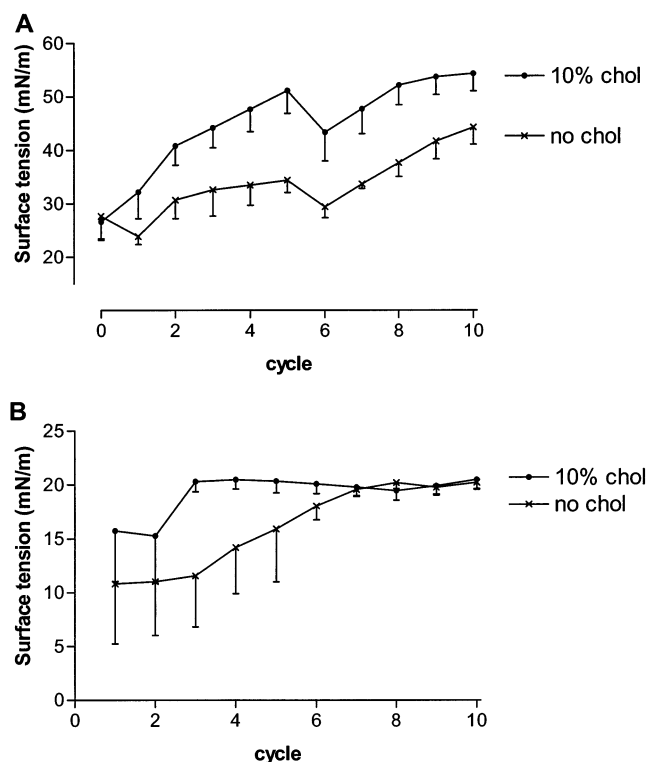


FIGURE 3: Maximum (A) and minimum (B) surface tensions during cycling of spread SP-C-containing lipid films, with and without 10% cholesterol (chol). The SP-C content of the mixture was 3 mol %. The lipids consisted of the standard phospholipid mixture DPPC/POPC/POPG (50/30/20), which was mixed with 100 mol % cholesterol to achieve the mol % cholesterol indicated. SUV and film had the same lipid composition. Values shown are the average of at least four separate experiments \pm SEM.

surface tension observed for the standard phospholipid mixture without cholesterol ($P = 0.017$), although there is an equal amount of DPPC in both mixtures. When maximum surface tension was measured, however, no statistically significant difference was found between the standard phospholipid mixture without cholesterol and the 50/10/20/20 mixture (Figure 2A). From the experiment described in Figure 2B it can be concluded that the increase in the minimum surface tension as a result of the addition of 20% cholesterol (Figure 1B) can be attributed not only to a lowering of the amount of DPPC in the lipid mixture but also partly to the added cholesterol itself.

Effect of Cholesterol in the Presence of SP-C. The presence of 10 mol % cholesterol in SP-C-containing films led to a significant increase of the maximum surface tension ($P = 0.033$) (Figure 3A). The minimum surface tension (Figure 3B) reached by these films was high (>10 mN/m) and tended toward the equilibrium surface tension (approximately 25 mN/m; 40) during cycling, indicating an irreversible loss of active material from the surface film into the subphase. There was no statistically significant difference in minimum surface tension reached between films with and without cholesterol.

Effect of Cholesterol in the Presence of both SP-B and SP-C. Interestingly, the presence of 10 mol % cholesterol had no effect on minimum or maximum surface tension when both SP-B and SP-C were present in the film (Figure 4). Moreover, compared to films containing either SP-B or SP-C (Figures 1 and 3), films containing both proteins had lower

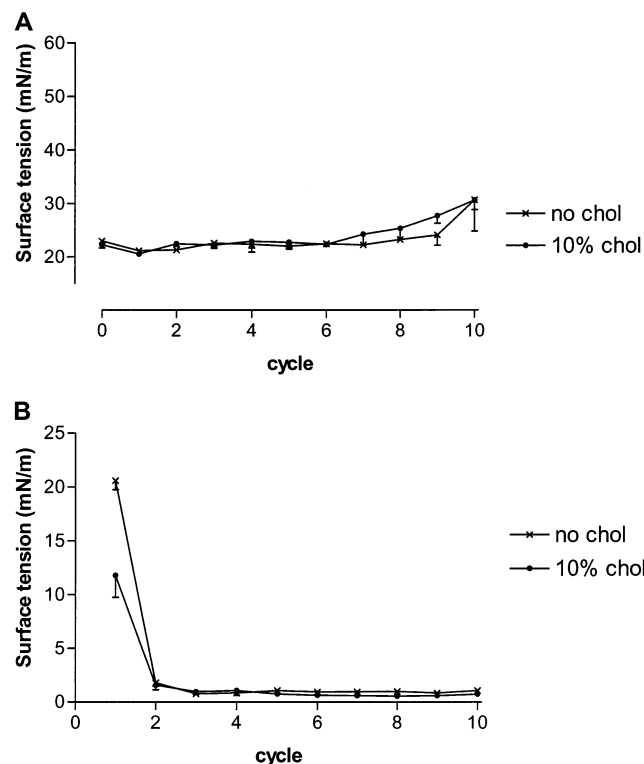


FIGURE 4: Maximum (A) and minimum (B) surface tensions during cycling of spread SP-B- and SP-C-containing lipid films, with and without 10% cholesterol (chol). The SP-B content of the mixture was 0.75 mol %; the SP-C content was 3 mol %. The lipids consisted of the standard phospholipid mixture DPPC/POPC/POPG (50/30/20), which was mixed with 100 mol % cholesterol to achieve the mol % cholesterol indicated. SUV and film had the same lipid composition. Values shown are the average of at least four separate experiments \pm SEM.

minimum surface tensions and did not show an increase of maximum surface tension during cycling.

Effect of Cholesterol in the Absence of Proteins. Both with and without cholesterol in the film, maximum surface tension in the absence of proteins rose to 59 mN/m at the first bubble expansion and leveled off at 65 mN/m on the third expansion (not shown). Furthermore, minimum surface tension reached with repeated film compression was never lower than the equilibrium surface tension, independent of the presence of cholesterol. So the presence of SP-B and/or SP-C is a requirement for obtaining and sustaining low maximum and minimum surface tension in this lipid mixture.

Effect of Cholesterol on Lipid Adsorption. To learn more about the processes during adsorption, the change in surface tension after sudden bubble expansion was recorded over a 5 s period. In the presence of SP-B, surface tensions observed before expansion were significantly lower in films containing 10 mol % cholesterol than in films without cholesterol (Figure 5A). Even though films with cholesterol appeared to reach a higher surface tension than films without cholesterol 1 s after bubble expansion, this difference was not statistically significant. Although films containing SP-C as the only protein started at similar surface tensions independent of cholesterol concentration (Figure 5B), the surface tension of films containing cholesterol rapidly rose to high values. The lowest surface tension was reached when both SP-B and SP-C were present, in both the presence and absence of cholesterol (Figure 5C). In the absence of proteins,

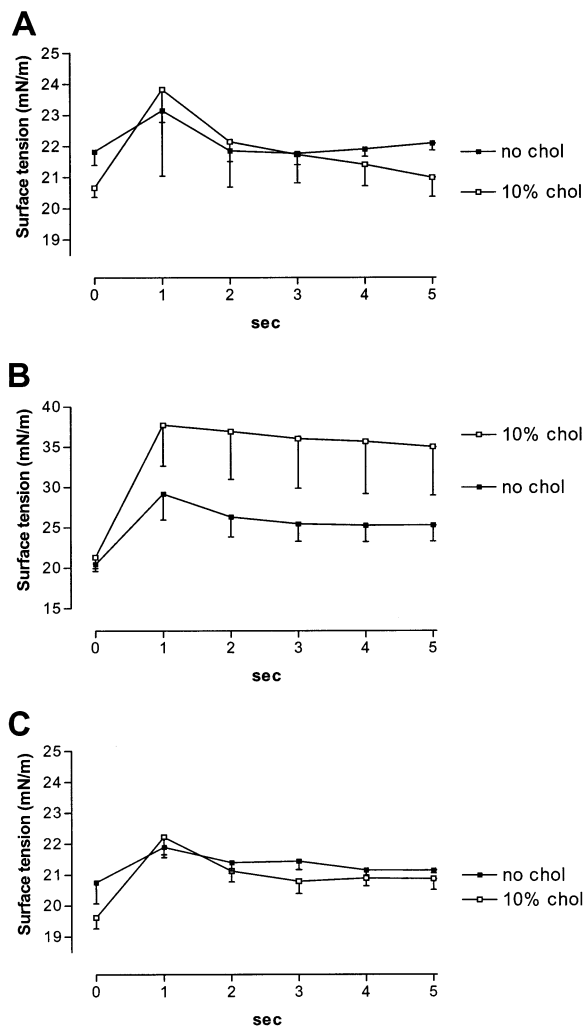


FIGURE 5: Adsorption during the first 5 s after sudden bubble expansion for lipid films, with and without 10% cholesterol (chol), containing SP-B (A), SP-C (B), or SP-B plus SP-C (C). The SP-B content of the mixture was 0.75 mol %; the SP-C content was 3 mol %. The lipids consisted of the standard phospholipid mixture DPPC/POPC/POPG (50/30/20), which was mixed with 100 mol % cholesterol to achieve the mol % cholesterol indicated. SUV and film had the same lipid composition. Values shown are the average of at least four separate experiments \pm SEM.

the surface tension of films with or without cholesterol rose quickly from 25 to 59 mN/m within the first second and remained at that level (not shown). No extra information was obtained when adsorption was viewed frame-by-frame (25 video frames per second) instead of second-by-second.

Effect of Cholesterol on Surface Film Topography: Atomic Force Microscopy

To determine whether the addition of cholesterol would influence the phase transition surface tensions and to determine a surface tension that would be suitable for film transfer, surface tension–area isotherms were made (Figure 6). From this figure it is clear that there is little or no difference between isotherms of mixtures containing and of those lacking cholesterol, so there are no indications for cholesterol-induced changes in phase transition surface tension. A typical feature of SP-B-containing films (Figure 6A,C) is a plateau in the isotherms at a surface tension of 32 mN/m. This plateau has also been found by others for

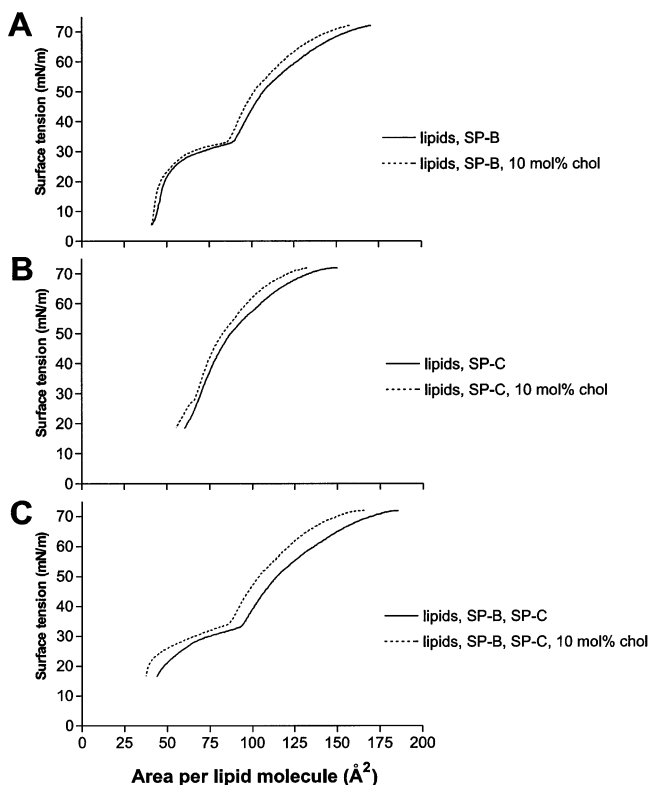


FIGURE 6: Surface tension–area isotherms of lipid films containing SP-B (A), SP-C (B), or SP-B plus SP-C (C), with and without 10 mol % cholesterol (chol). The SP-B content of the mixture was 0.75 mol %; the SP-C content was 3 mol %. The lipids consisted of the standard phospholipid mixture DPPC/POPC/POPG (50/30/20), which was mixed with 100 mol % cholesterol to achieve the mol % cholesterol indicated. Compression isotherms were made on a water subphase at 21 °C.

SP-B in DPPC/DPPG (4/1 v/v) (41) or SP-B/cholesterol mixtures (26) and is indicative of squeeze-out of surfactant material from the monolayer. For films containing SP-C as the sole protein (Figure 6B), squeeze-out is not readily visible in the absence of cholesterol, but an indication of squeeze-out (starting at a surface tension of approximately 27 mN/m) is observed in its presence. To obtain additional information about film structure below the equilibrium surface tension and to compare it with results of other studies (1, 41), surfactant films were compressed to a surface tension of 22 mN/m, since it can be concluded from Figure 6 that squeeze-out has already begun at this surface tension. Films were composed of the standard phospholipid mixture plus SP-B, SP-C, or both proteins. Cholesterol was present in the films at a concentration of 0 or 10 mol %. In AFM and fluorescence microscopy studies dealing with SP-B and SP-C in DPPC/DPPG mixtures, it was shown that at a surface tension of 22 mN/m protrusions (white regions in the AFM images) contained lipid and protein in liquid expanded phase, while the monolayer (black regions in the AFM images) consisted solely of lipid in liquid condensed phase (1, 41, 42).

Representative $10\ \mu\text{m} \times 10\ \mu\text{m}$ AFM scans of mica-supported DPPC/POPC/POPG films with SP-B and/or SP-C are shown in Figures 7–9, in both the absence and presence of cholesterol. For SP-B-containing films the surface topography dramatically differed between films containing 0% or 10% cholesterol (Figure 7). In the absence of cholesterol,

continuous network structures were present, appearing as mountain ridges. Since addition of more surfactant proteins led to the formation of a larger amount of protrusions, we deduce, analogous to the work of Amrein, Sieber, and co-workers (1, 41, 42), that the protrusions consist of protein and lipid. AFM allows very accurate measurements in the z direction, i.e., height. The height of the protein/lipid protrusions was almost exclusively 24 ± 3 nm. Since the shape of each individual AFM tip [up to 10 nm at the apex (43), 50 nm in radius (44)] is not known exactly, AFM does not allow very accurate measurements (tip convolution) in the x and y direction, i.e., protrusion widths. Nevertheless, widths of similar samples scanned with the same tip can be roughly compared with each other. The width of the ridges ranged between 100 and 400 nm and were approximately 200 nm on average. In contrast, films containing 10% cholesterol showed noncontinuous networks made up of small domains such as pearls-on-a-string, with a height of typically 13 ± 2 nm. The average size of the protrusions (i.e., the separate pearls on the string) was roughly 100 nm.

For SP-C-containing films the difference in topography was less extreme than for films containing SP-B, but the same trend was observed: in cholesterol-containing films the protrusions seemed to be homogeneously dispersed (Figure 8B), while films without cholesterol also contained lipid areas without protrusions (Figure 8A, e.g., upper part in the center). In both the presence and absence of cholesterol the height of the protrusions was 4 ± 1 nm. Incidentally, a height of 8 nm was observed. The shape of the protrusions was mostly noncircular. The size of the protrusions varied largely, being 100 nm on average, and was independent of the presence of cholesterol.

The structure of films containing both SP-B and SP-C was a combination of the film topography observed in the presence of the separate proteins (compare Figure 9 with Figures 7 and 8). In the absence of cholesterol there is a striking pattern of monolayer surrounded by many circular protrusions of lipids/proteins. This pattern is absent in the presence of cholesterol, although incidentally a region was found that contained both unorganized and organized structures. In the absence of cholesterol the height of the protrusions varied, ranging from 16 to 24 nm in steps of 4 nm, while in the presence of cholesterol higher protrusions of up to 34 nm were also found. The size of the protrusions (i.e., the separate pearls on the string) were approximately 100 nm, independent of the presence of cholesterol.

When no proteins were present, no differences in topography were found between the standard phospholipid mixture plus or minus cholesterol. The surfaces of these films were predominantly flat (results not shown). No phase separation was observed.

When the amount of white (protrusions) of the AFM images was determined, it was found that the total area of protrusions in SP-B films was significantly higher ($P < 0.001$) in the presence of cholesterol ($15.6\% \pm 1.0\%$) than in its absence ($12.3\% \pm 1.3\%$). In the case of SP-C a similar trend (but not statistically significant) was observed: $8.7\% \pm 1.4\%$ in the presence and $7.2\% \pm 2.0\%$ in the absence of cholesterol. However, when both proteins were present in the film, the total area of protrusions was lower in the presence ($19.1\% \pm 8.8\%$) than in the absence ($25.9\% \pm 6.5\%$) of cholesterol ($P = 0.031$).

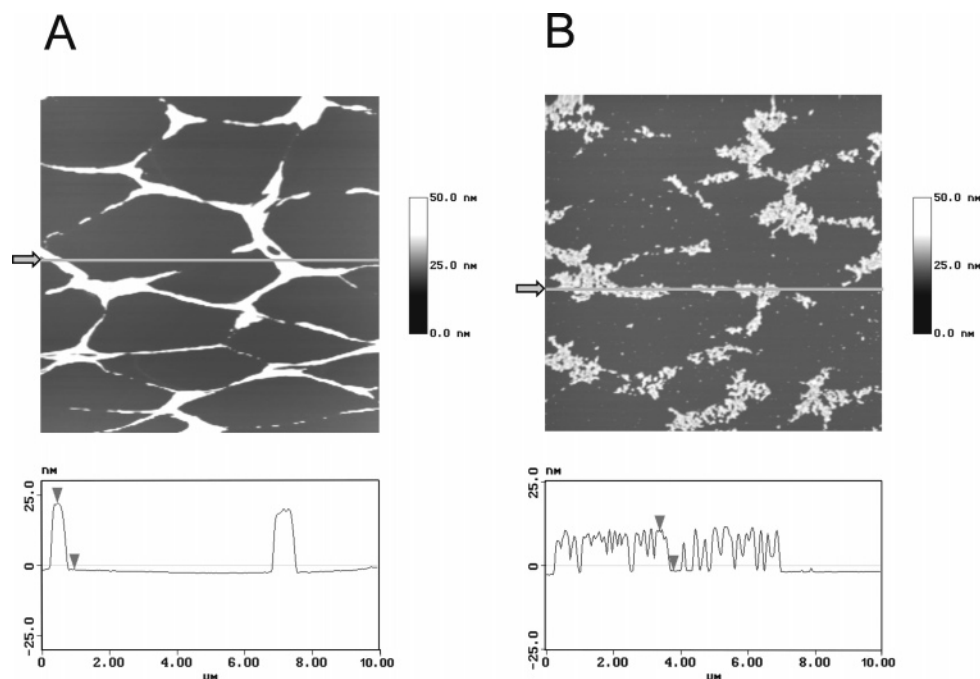


FIGURE 7: AFM topography of SP-B-containing lipid films, without (A) and with (B) 10 mol % cholesterol. The SP-B content of the mixture was 0.75 mol %. The lipids consisted of the standard phospholipid mixture DPPC/POPC/POPG (50/30/20), which was mixed with 100 mol % cholesterol to achieve the mol % cholesterol indicated. Black regions represent lipid monolayer, while white regions are protrusions of lipids/protein. The average height of the protrusions was 24 ± 3 nm for panel A and 13 ± 2 nm for panel B. The arrowheads on the height traces show the approximate height difference, which was 23.9 nm for panel A and 12.1 nm for panel B. Scan area was $10 \mu\text{m} \times 10 \mu\text{m}$.

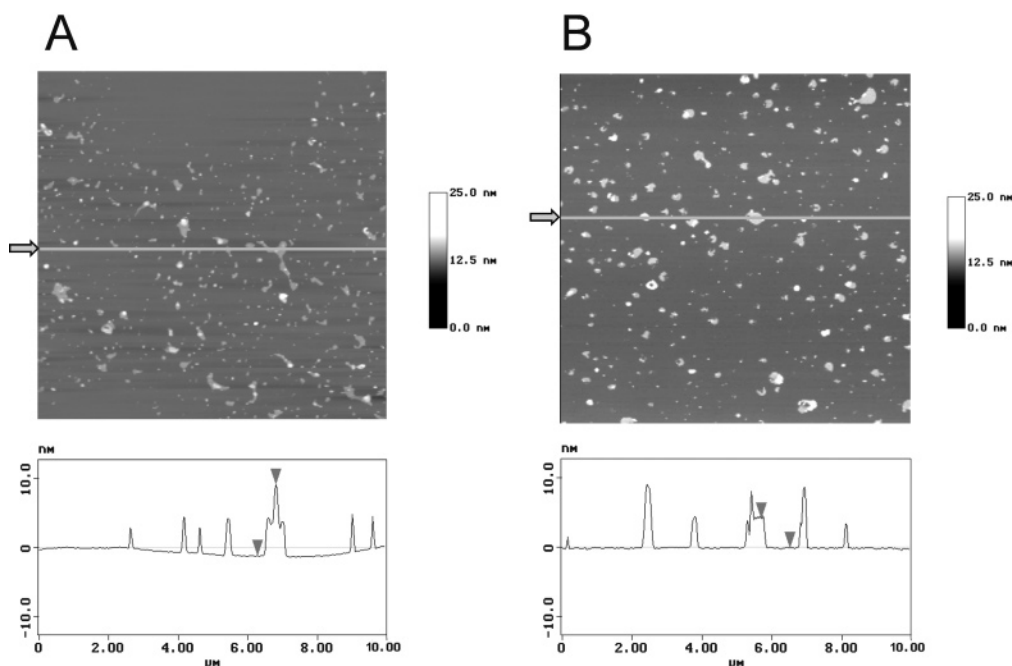


FIGURE 8: AFM topography of SP-C-containing lipid films, without (A) and with (B) 10 mol % cholesterol. The SP-C content of the mixture was 3 mol %. The lipids consisted of the standard phospholipid mixture DPPC/POPC/POPG (50/30/20), which was mixed with 100 mol % cholesterol to achieve the mol % cholesterol indicated. The average height of the protrusions was typically 4 ± 1 nm for both panels, but protrusions of 8 nm height were observed as well. The arrowheads on the height traces show the approximate height difference, which was 8.8 nm for panel A and 4.1 nm for panel B. Scan area was $10 \mu\text{m} \times 10 \mu\text{m}$.

DISCUSSION

Approximately 10–20 mol % of the surfactant lipids are nonphospholipid. However, the exact function of these neutral lipids (mainly cholesterol) in surfactant is not clear. In general, cholesterol is able to induce the liquid ordered phase, in which lipid acyl chains are extended and tightly packed as in the solid phase, although the lateral diffusion

is almost as high as in the fluid phase. In this way cholesterol increases the fluidity of the lipid acyl chains below the transition temperature of that lipid but rigidifies the acyl chains above the transition temperature (24, 45). The greatest rigidifying effect is exerted on fully saturated PC, with cholesterol packing in the intermolecular cavities of DPPC (46), and the least on PC containing a double bond in both

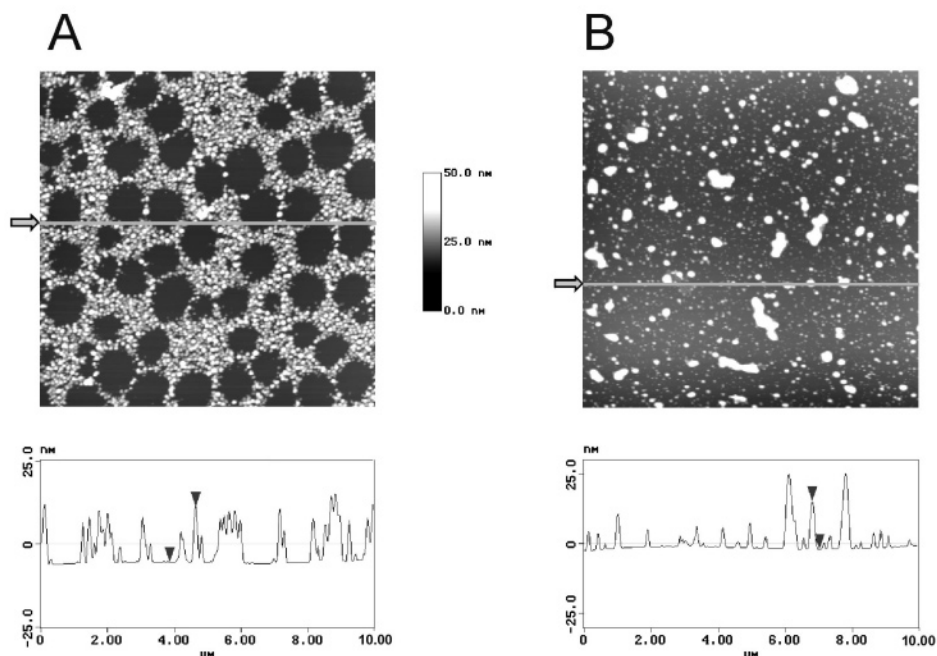


FIGURE 9: AFM topography of SP-B- and SP-C-containing lipid films, without (A) and with (B) 10 mol % cholesterol. The SP-B content of the mixture was 0.75 mol %; the SP-C content was 3 mol %. The lipids consisted of the standard phospholipid mixture DPPC/POPC/POPG (50/30/20), which was mixed with 100 mol % cholesterol to achieve the mol % cholesterol indicated. Heights of the protrusions ranged from 16 to 24 nm in steps of 4 nm in the absence of cholesterol (A). In the presence of cholesterol heights ranging from 16 to 34 nm in steps of 4 nm were found (B). The arrowheads on the height traces show the approximate height difference, which were 16.3 nm for panel A and 16.6 nm for panel B. Scan area was $10\ \mu\text{m} \times 10\ \mu\text{m}$.

acyl chains (47). The fluidizing effect is achieved by direct interaction of cholesterol with the fatty acyl chains of the phospholipids, preventing them from crystallizing by coming too close together, thereby preventing possible phase transitions. In surfactant at physiological temperature, cholesterol is thought to act as a fluidizing agent, enhancing adsorption and respreading of lipid from collapsed phase (28, 48). This study shows that there is an ideal cholesterol concentration of around 10 mol % for SP-B-containing surfactant films. Furthermore, cholesterol was found to induce dramatic structural alterations in films containing SP-B and/or SP-C.

In our CBS experiments, cholesterol lowered maximum surface tension in the presence of SP-B. This effect was dependent on cholesterol concentration. On one hand, too much cholesterol in the film destabilized the monolayer, preventing the film from reaching low minimum surface tensions (Figure 1B). This is likely due to the fact that the cholesterol concentration in the film was higher than a critical level at which it can no longer be squeezed out rapidly, as was observed in DPPC/cholesterol monolayers (49). On the other hand, a total absence of cholesterol led to a rise in minimum surface tension after six bubble compressions. Therefore, it is conceivable that the presence of cholesterol has a beneficial effect on film stability by packing between the fatty acyl chains of DPPC, leading to an improved tolerance of high lateral pressures. Furthermore, maximum surface tension decreased with increasing cholesterol concentration, reaching the lowest value at 10 mol % in the presence of SP-B. These findings are different from those obtained in a PBS study (27) on DPPC/POPG/SP-B (70/30/0.4 mol/mol/mol) where both minimum and maximum surface tension were found to be higher after addition of 20 mol % cholesterol. In another study, with the Wilhelmy balance, cholesterol (up to 10 mol %) in the presence of

SP-B increased minimum surface tension as well (25). Surprisingly, we found that cholesterol increased both maximum and minimum surface tension in films containing SP-C (Figure 3). One could speculate that cholesterol at this concentration fixes the orientation of the SP-C palmitoyl chains in the membrane, thereby decreasing the freedom to move between lipid layers of the surface-associated reservoir and altering the monolayer lipid composition. It is thought that SP-C is more favorably accommodated in fluid DPPC bilayers than in rigid gel-phase DPPC (50, 51). Furthermore, in the presence of cholesterol, SP-C-containing films did not reach the same low surface tensions as films with SP-B. This is in line with another CBS study (37) in which it was shown that SP-C had less of a refining effect on surfactant films than SP-B. Thus, in the presence of SP-B the effect of cholesterol on surface activity is the opposite of that found for SP-C. When both SP-C and SP-B were present in the film, an overall improvement on surface activity compared to that in the presence of either protein separately was obtained (compare Figure 4 with Figures 1 and 3) on which cholesterol addition had no effect. In our experiments performed at 37 °C only minor effects of cholesterol on adsorption were seen (Figure 5), although the CBS method with spread films is accurate enough to measure small differences in surface tension. Moreover, the influence of surfactant proteins on adsorption seemed much more pronounced than the influence of cholesterol. Yet, in a study that employed a Wilhelmy balance as well as a PBS, both at 37 and at 23 °C, calf lung surfactant extract devoid of neutral lipids was reported to have hampered adsorption activity (higher maximum surface tensions) compared with complete calf lung surfactant extract (52). In the same study neutral lipids were also reported to facilitate respreading. As leakage of film material is a problem often encountered in

experiments with the PBS or the Wilhelmy balance (23, 33, 35), some of the detrimental effects attributed to cholesterol may instead have been related to film leakage.

When spread films on a Langmuir–Wilhelmy balance are compressed beyond the equilibrium surface tension, surfactant components leave the interface, forming structures connected to the monolayer. Therefore, parts of the film must undergo transformation from a monolayer into structures protruding into or out of the aqueous subphase. Other studies with fluorescence microscopy, time-of-flight secondary ion mass spectrometry, and Brewster angle microscopy showed that structures transferred from the air/water interface onto solid substrates are essentially identical to the structures in the monolayer itself (53, 54). To achieve a better understanding of the effect of cholesterol on formation of such structures, we used AFM to study, for the first time, surfactant films containing cholesterol that were compressed below the equilibrium surface tension. The most striking difference between AFM images of films containing and those lacking cholesterol is that protrusions in the presence of cholesterol appear more dispersed throughout the entire area and less clustered into network structures (Figures 7–9). This homogenizing effect of cholesterol was observed for films containing SP-B, SP-C, and both proteins.

In our AFM studies protrusion heights were often multiples of 4–4.5 nm, independent of the presence of cholesterol. The value found for bilayer height depends on method of analysis, temperature, and lipid unsaturation. The bilayer thickness of DPPC was found to be 3.7 nm (55) to 4.3 nm (56) in fluid liquid crystalline state and 4.7 nm in gel state (56), as determined by X-ray diffraction. In an AFM study in contact mode, films of SP-B in DPPC/DPPG (4/1) transferred at 22 mN/m were found to have protrusions of 6–7 nm, thought to represent bilayers (41). However, in another AFM study in contact mode, protrusions in films of SP-B peptide analogues in DPPG/POPG (3/1) transferred at 18 mN/m were found to be 10–40 nm, in steps of 5.0 nm (57). Therefore, in our study we considered a height of 4–4.5 nm to represent the thickness of a bilayer. Thus, most protrusions found in films with SP-C were 1 bilayer in thickness, while those found in SP-B-containing films were 3–6 bilayers thick. This finding is different from the scarce AFM information available on films containing SP-B or SP-C, since compression of films containing DPPC/DPPG (4/1) plus SP-C was found to result in the formation of protrusions with a height of multiples of bilayers (1), while the same lipid mixture plus SP-B resulted in protrusions of only one bilayer in thickness (41). In line with our results, multilayered structures were found for SP-B analogues in DPPG/POPG (57). The discrepancy between results is likely to be due to the differences in lipid mixtures used. Our highly unsaturated lipid mixture presumably led to altered fluidity and thereby to a different tendency to form protrusions during squeeze-out of film components. Unfortunately, the methods used in our studies do not provide information on whether cholesterol is present in the protrusions or located between DPPC in the condensed lipid domains.

Extrapolation of our AFM findings to the physiological situation is difficult since surface tension in the lung can reach a value down to 9 mN/m (58), while the surface tensions that we could achieve in the Langmuir–Wilhelmy balance during film transfer ranged from 15 to 72 mN/m.

Nevertheless, it is of interest that a dramatic alteration in surface topography like that observed after addition of cholesterol to films containing both SP-B and SP-C is not accompanied by measurable differences in surface activity in the CBS. Apparently, both types of structures allow rapid insertion and removal of lipids in to and out of the monolayer. An explanation might be the small domain sizes of liquid expanded phase in both structures. From the broad and continuous network structures seen in the absence of cholesterol in films containing SP-B as the only protein (Figure 7A), it is apparently more difficult to insert lipids into an expanding bubble, since maximum surface tension increases as cholesterol concentration decreases (Figure 1A).

In summary, it is shown that cholesterol lowers the maximum surface tension in SP-B-containing films. This result, combined with the AFM data, indicates that in the presence of SP-B the cholesterol-induced organization of the surfactant reservoir in smaller units leads to facilitated lipid spreading during bubble area increase. In the presence of SP-C, however, the dispersing effect of cholesterol is hardly detectable by AFM, while cholesterol causes an increased maximum surface tension in the CBS, indicating that deleterious effects such as decreased freedom of movement of SP-C prevail. When the film contains both SP-B and SP-C the homogenizing effect of cholesterol is present, but apparently this positive effect that cholesterol has in the presence of SP-B is abolished by the deleterious effect that cholesterol has in the presence of SP-C. Moreover, our CBS data provide additional evidence for the general concept that natural surfactant containing SP-B and SP-C is superior to surfactants lacking one of these components. Although the lipid mixture used in the present investigations is simpler than the composition of natural surfactant, the observation that, in the presence of both SP-B and SP-C, cholesterol has no effect on the surface activity of the surfactant under dynamic conditions raises the possibility that the cholesterol found in surfactant of warm-blooded mammals does not have a function in surface activity. The function of a membrane fluidizer could instead be achieved by lipids containing unsaturated fatty acids. Cholesterol may be present in surfactant to fulfill another important role, for instance, as an antioxidant (59). Alternatively, it cannot be excluded that the presence of cholesterol in the surfactant of homeothermic endotherms is an evolutionary relic. This would be in line with the observation that throughout the evolution of vertebrates, from fish through amphibians and reptiles to mammals, the relative proportion of cholesterol decreases, whereas that of the saturated phospholipids increases (24).

REFERENCES

1. Amrein, M., von Nahmen, A., and Sieber, M. (1997) *Eur. Biophys. J.* 26, 349–357.
2. Schürch, S., Qanbar, R., Bachofen, H., and Possmayer, F. (1995) *Biol. Neonate* 67 (Suppl. 1), 61–76.
3. Bangham, A. D., Morley, C. J., and Phillips, M. C. (1979) *Biochim. Biophys. Acta* 573, 552–556.
4. Clements, J. A. (1977) *Am. Rev. Respir. Dis.* 115, 67–71.
5. Crane, J. M., and Hall, S. B. (2001) *Biophys. J.* 80, 1863–1872.
6. Lipp, M. M., Lee, K. Y. C., Takamoto, D. Y., Zasadinski, J. A., and Waring, A. J. (1998) *Phys. Rev. Lett.* 81, 1650–1653.
7. Hawgood, S., Benson, B. J., Schilling, J., Damm, D., Clements, J. A., and White, R. T. (1987) *Proc. Natl. Acad. Sci. U.S.A.* 84, 66–70.

8. Yu, S. H., and Possmayer, F. (1992) *Biochim. Biophys. Acta* 1126, 26–34.
9. Pérez-Gil, J., Casals, C., and Marsh, D. (1995) *Biochemistry* 34, 3964–3971.
10. Baatz, J. E., Elledge, B., and Whitsett, J. A. (1990) *Biochemistry* 29, 6714–6720.
11. Oosterlaken-Dijksterhuis, M. A., Haagsman, H. P., van Golde, L. M. G., and Demel, R. A. (1991) *Biochemistry* 30, 8276–8281.
12. Taneva, S. G., and Keough, K. M. W. (1994) *Biochemistry* 33, 14660–14670.
13. Poulain, F. R., Allen, L., Williams, M. C., Hamilton, R. L., and Hawgood, S. (1992) *Am. J. Physiol.* 262, L730–L739.
14. Suzuki, Y., Fujita, Y., and Kogishi, K. (1989) *Am. Rev. Respir. Dis.* 140, 75–81.
15. Horowitz, A. D., Moussavian, B., and Whitsett, J. A. (1996) *Am. J. Physiol.* 270, L69–L79.
16. Veldhuizen, E. J. A., Batenburg, J. J., van Golde, L. M. G., and Haagsman, H. P. (2000) *Biophys. J.* 79, 3164–3171.
17. Clark, J. C., Wert, S. E., Bachurski, C. J., Stahlman, M. T., Stripp, B. R., Weaver, T. E., and Whitsett, J. A. (1995) *Proc. Natl. Acad. Sci. U.S.A.* 92, 7794–7798.
18. Robertson, B., Kobayashi, T., Ganzuka, M., Grossmann, G., Li, W. Z., and Suzuki, Y. (1991) *Pediatr. Res.* 30, 239–243.
19. Johansson, J., Szyperski, T., Curstedt, T., and Wüthrich, K. (1994) *Biochemistry* 33, 6015–6023.
20. Curstedt, T., Jörnvall, H., Robertson, B., Bergman, T., and Berggren, P. (1987) *Eur. J. Biochem.* 168, 255–262.
21. Qanbar, R., Cheng, S., Possmayer, F., and Schürch, S. (1996) *Am. J. Physiol.* 271, L572–L580.
22. Glasser, S. W., Burhans, M. S., Korfhagen, T. R., Na, C. L., Sly, P. D., Ross, G. F., Ikegami, M., and Whitsett, J. A. (2001) *Proc. Natl. Acad. Sci. U.S.A.* 98, 6366–6371.
23. Veldhuizen, R. A., Nag, K., Orgeig, S., and Possmayer, F. (1998) *Biochim. Biophys. Acta* 1408, 90–108.
24. Orgeig, S., and Daniels, C. B. (2001) *Comp. Biochem. Physiol. A* 129, 75–89.
25. Suzuki, Y. (1982) *J. Lipid Res.* 23, 62–69.
26. Taneva, S. G., and Keough, K. M. W. (1997) *Biochemistry* 36, 912–922.
27. Yu, S. H., and Possmayer, F. (1994) *Biochim. Biophys. Acta* 1211, 350–358.
28. Notter, R. H., Tabak, S. A., and Mavis, R. D. (1980) *J. Lipid Res.* 21, 10–22.
29. Oosterlaken-Dijksterhuis, M. A., Haagsman, H. P., van Golde, L. M. G., and Demel, R. A. (1991) *Biochemistry* 30, 10965–10971.
30. Böhlen, P., Stein, S., Dairman, W., and Udenfriend, S. (1973) *Arch. Biochem. Biophys.* 155, 213–220.
31. Rouser, G., Fleischer, S., and Yamamoto, A. (1970) *Lipids* 5, 494–496.
32. Allain, C. C., Poon, L. S., Chan, C. S., Richmond, W., and Fu, P. C. (1974) *Clin. Chem.* 20, 470–475.
33. Putz, G., Goerke, J., Schürch, S., and Clements, J. A. (1994) *J. Appl. Physiol.* 76, 1417–1424.
34. Putz, G., Walch, M., van Eijk, M., and Haagsman, H. P. (1998) *Biophys. J.* 75, 2229–2239.
35. Putz, G., Goerke, J., Taeusch, H. W., and Clements, J. A. (1994) *J. Appl. Physiol.* 76, 1425–1431.
36. Diemel, R. V., Bader, D., Walch, M., Hotter, B., van Golde, L. M. G., Amann, A., Haagsman, H. P., and Putz, G. (2001) *Arch. Biochem. Biophys.* 385, 338–347.
37. Veldhuizen, E. J. A., Diemel, R. V., Putz, G., van Golde, L. M. G., Batenburg, J. J., and Haagsman, H. P. (2001) *Chem. Phys. Lipids* 110, 47–55.
38. Putz, G., Walch, M., van Eijk, M., and Haagsman, H. P. (1999) *Biochim. Biophys. Acta* 1453, 126–134.
39. Holm, B. A., Wang, Z., Egan, E. A., and Notter, R. H. (1996) *Pediatr. Res.* 39, 805–811.
40. Goerke, J., and Clements, J. A. (1986) in *Handbook of Physiology—The Respiratory System* (Macklem, P. T., and Mead, J., Eds.) pp 247–261, American Physiological Society, Bethesda, MD.
41. Krol, S., Ross, M., Sieber, M., Kunneke, S., Galla, H.-J., and Janshoff, A. (2000) *Biophys. J.* 79, 904–918.
42. von Nahmen, A., Schenk, M., Sieber, M., and Amrein, M. (1997) *Biophys. J.* 72, 463–469.
43. Sheng, S., Czajkowsky, D. M., and Shao, Z. (1999) *J. Microsc.* 196, 1–5.
44. Zasadzinski, J. A., Helm, C. A., Longo, M. L., Weisenhorn, A. L., Gould, S. A., and Hansma, P. K. (1991) *Biophys. J.* 59, 755–760.
45. McElhaney, R. N. (1982) *Chem. Phys. Lipids* 30, 229–259.
46. Shah, D. O., and Schulman, J. H. (1967) *J. Lipid Res.* 8, 215–226.
47. Guyer, W., and Bloch, K. (1983) *Chem. Phys. Lipids* 33, 313–322.
48. Daniels, C. B., Barr, H. A., Power, J. H., and Nicholas, T. E. (1990) *Exp. Lung Res.* 16, 435–449.
49. Yu, S. H., and Possmayer, F. (1998) *J. Lipid Res.* 39, 555–568.
50. Johansson, J., Szyperski, T., and Wüthrich, K. (1995) *FEBS Lett.* 362, 261–265.
51. Johansson, J. (1998) *Biochim. Biophys. Acta* 1408, 161–172.
52. Wang, Z., Hall, S. B., and Notter, R. H. (1995) *J. Lipid Res.* 36, 1283–1293.
53. Galla, H.-J., Bourdos, N., von Nahmen, A., Amrein, M., and Sieber, M. (1998) *Thin Solid Films* 327, 632–635.
54. Bourdos, N., Kollmer, F., Benninghoven, A., Ross, M., Sieber, M., and Galla, H.-J. (2000) *Biophys. J.* 79, 357–369.
55. Lewis, B. A., and Engelman, D. M. (1983) *J. Mol. Biol.* 166, 211–217.
56. Marsh, D. (1990) *Handbook of lipid bilayers*, Chemical Rubber Co., Boca Raton, FL.
57. Takamoto, D. Y., Lipp, M. M., von Nahmen, A., Lee, K. Y., Waring, A. J., and Zasadzinski, J. A. (2001) *Biophys. J.* 81, 153–169.
58. Schürch, S., Goerke, J., and Clements, J. A. (1976) *Proc. Natl. Acad. Sci. U.S.A.* 73, 4698–4702.
59. Parasassi, T., Giusti, A. M., Raimondi, M., Ravagnan, G., Sapora, O., and Gratton, E. (1995) *Free Radic. Biol. Med.* 19, 511–516.

BI0256532